Covert Communication for Jammer-aided Multi-Antenna UAV Networks

Hongyang Du, Dusit Niyato, *Fellow, IEEE*, Yuan-ai Xie, Yanyu Cheng, Jiawen Kang*, and Dong In Kim, *Fellow, IEEE*

***Abstract*—Unmanned aerial vehicles (UAVs) have attracted a lot of research attention in serving as aerial base stations (BSs). To protect the data privacy without being detected by a warden, we investigate a jammer-aided UAV covert communication system, aiming to maximize the user's covert rate with optimized transmit and jamming power. By considering the general composite fading and shadowing channel models, we derive the closed-form expressions for detection error probability and covert rate. The covert rate maximization problem is formulated as a Nash bargaining game, and the Nash bargaining solution (NBS) is introduced. To solve the NBS, we propose a particle swarm optimization-based power allocation algorithm. The numerical results are presented to verify the theoretical analysis.**

***Index Terms*—Covert communication, multi-antenna UAV, performance analysis, optimization, Bargaining game.**

I. Introduction

Wireless communication networks have always required a high data rate and secure transmission. As sixth-generation networks aspire for higher capacity and lower latency, the number of mobile users and devices is rapidly rising. Thus, common ground base stations (BSs) may be unable to cover all Internet-of-things (IoT) devices and gather data effectively. As a result, a new paradigm is urgently required to enhance the cellular network's quality of service (QoS).

Because of the flexible operation and large coverage, unmanned aerial vehicle (UAV)-aided communications are regarded as one of the most promising techniques for future networks [1]. However, several challenges still exist. For example, the wide coverage and large-scale connection of UAVs, make the open networks vulnerable to eavesdropping or various attacks by malicious adversaries [2]. Since UAVs are commonly used to transmit private data, it is critical to design a secure UAV-aided system. Fortunately, the covert communication technique can effectively not only protect the contents, but also hide the transmission behavior.

To degrade the warden's detection performance, a friendly jammer is introduced. Subject to the power constraints, the jammer aims to use less power to help each user, which impel us to study how users bargain and negotiate with each other to achieve their covert communication. Hence, it is natural to apply game theory to balance the objectives among different pairs [3]. Thus, a Nash bargaining approach is proposed to obtain the Nash bargaining solution (NBS) [4]. An agreement can be achieved by players, i.e., K users, efficiently and fairly, given the NBS's five axioms of pareto optimality (PAR), individual rationality (IR), independent of expected utility representations (INV), independence of irrelevant alternatives (IIA) and symmetry (SYM) [4].

In this paper, we investigate a jammer-aided multi-antenna UAV covert communication system. The main contributions are summarized as follows:

- By modeling the ground channel links as Fisher-Snedecor $\mathcal{F}$ fading and the air-to-ground channel links as Fluctuating Two-Ray (FTR) fading, the detection error probability and covert rate are derived.
- To maximize the covert rate with limited transmit and jamming power, the problem is formulated as a Nash bargaining game (NBG). Furthermore, the NBS is introduced to investigate the negotiation among K users. We propose a particle swarm optimization (PSO)-based power allocation (PPA) algorithm, to solve the formulated problem. A detection error probability minimization algorithm of the warden is also proposed.

Mathematical Notations and Functions: $\Pr\{\cdot\}$ is probability function, $\boldsymbol{a}^T$ denotes transpose of vector $\boldsymbol{a}$. In FTR fading model, K is the average power ratio of the dominant wave to the scattering multipath, m_k and m_w are the fading severity parameter for the k_{th} user & warden, Δ_k and Δ_w are parameters varying from 0 to 1 representing the similarity of two dominant waves for the k_{th} user & warden, σ_k and σ_w are the standard deviation of the diffuse received signal component for the k_{th} user & warden, υ_k and υ_w are the received average SNR for the k_{th} user & warden. In Fisher-

This research is supported by NSFC under grant No. 62102099 and Key Project in Higher Education of Guangdong Province under grant No. 2020ZDZX3030. This research is also supported by, in part, the programme DesCartes and is supported by the National Research Foundation, Prime Minister's Office, Singapore under its Campus for Research Excellence and Technological Enterprise (CREATE) programme, Alibaba Group through Alibaba Innovative Research (AIR) Program and Alibaba-NTU Singapore Joint Research Institute (JRI), the National Research Foundation, Singapore under the AI Singapore Programme (AISG) (AISG2-RP-2020-019), and Singapore Ministry of Education (MOE) Tier 1 (RG16/20). (*Corresponding author: Jiawen Kang*).

H. Du is with the School of Computer Science and Engineering, the Energy Research Institute @ NTU, Interdisciplinary Graduate Program, Nanyang Technological University, Singapore (e-mail: hongyang001@e.ntu.edu.sg).

D. Niyato is with the School of Computer Science and Engineering, Nanyang Technological University, Singapore (e-mail: dniyato@ntu.edu.sg)

J. Kang is with the School of Automation, Guangdong University of Technology, China. (e-mail: kavinkang@gdut.edu.cn)

Yuan-ai Xie is with the Institute of Electrical Engineering, Yanshan University, China. (emails: xieyuan_ai@163.com)

Y. Cheng is with Alibaba-NTU Singapore Joint Research Institute, Nanyang Technological University, Singapore (e-mail: yanyu.cheng@ntu.edu.sg).

D. I. Kim is with the Department of Electrical and Computer Engineering, Sungkyunkwan University, South Korea (e-mail: dikim@skku.ac.kr)

Snedecor $\mathcal{F}$ fading model, $\upsilon = 2\sigma^2(1+K)$, m_{fk} and m_{fw} are the fading parameters for the k_{th} user & warden, m_{sk} and m_{sw} are the shadowing parameters for the k_{th} user & warden, $\bar{z}_k$ and $\bar{z}_w$ are the average value of $\mathcal{F}$ random variables (RVs). ${}_1F_1(\cdot;\cdot;\cdot)$ denotes the confluent hypergeometric function [5, eq. (9.210.1)], $\Gamma(z)$ is the Gamma function [5, eq. (8.310.1)], $\gamma(\cdot,\cdot)$ is the incomplete Gamma function [5, eq. (8.350.1)], $B(\cdot,\cdot)$ is the beta function [5, eq. (8.384.1)], ${}_2F_1(\cdot,\cdot;\cdot;\cdot)$ denotes the Gauss hypergeometric function [5, eq. (9.111)], $G_{p,q}^{m,n}(\cdot)$ is the Meijer's G-function [5, eq. (9.301)], and $G(\cdot)$ is the Bivariate Meijer's G-function [6, eq. (1)].

II. System Model and SINR Analysis

A. System Description

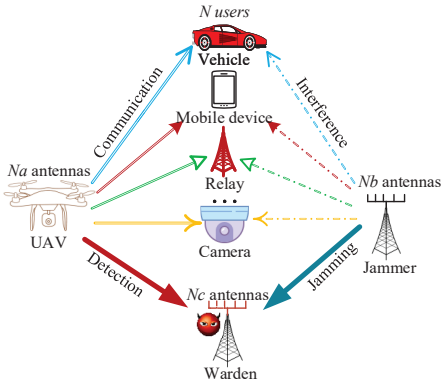

Fig. 1. A jammer-aided multi-antenna UAV covert communication system.

As shown in Fig. 1, we consider a jammer-aided multi-antenna UAV covert communication for K users. The UAV transmits the private data to the corresponding users simultaneously. To prevent private data transmission from being detected by a warden, a friendly jammer is used. We assume that all users are equipped with a single antenna. To avoid the interference among users, the UAV assigns different orthogonal frequency channels to use the k_{th} antenna to serve k_{th} user [1]. The jammer uses its k_{th} antenna to jam the k_{th} channel to interfere the warden's detection. The locations of the user U_k, the jammer, the UAV, and the warden can be expressed by $\mathbf{q}_k = [x_k, y_k, z_k]^T$ $(\forall k \in \mathcal{K})$, $\mathbf{q}_j = [x_j, y_j, z_j]^T$, $\mathbf{q}_a = [x_a, y_a, z_a]^T$ and $\mathbf{q}_w = [x_w, y_w, , z_w]^T$, respectively. Therefore, the distances from UAV to the user U_k and the warden, can be expressed as D_{ak} and D_{aw}, respectively, where $D_{ai} = \|\mathbf{q}_a - \mathbf{q}_i\|$ $(i = k, w)$. The distances from the jammer to the kth user and the warden are denoted by D_{jk} and D_{jw}, respectively, where $D_{ji} = \|\mathbf{q}_j - \mathbf{q}_i\|$.

B. Channel Model

We introduce the FTR and Fisher-Snedecor $\mathcal{F}$ fading models for the air-to-ground and ground-to-ground links, respectively. The reason is as follows:

- Recent small-scale fading measurements of the 28 GHz outdoor millimeter-wave channels [8] have shown that the FTR fading model can provide a significantly better match to the real channel than the Rician fading model.
- The Fisher-Snedecor $\mathcal{F}$ fading has been proven to give a more thorough modeling and characterization of the simultaneous occurrence of multipath fading and shadowing [9]. In addition, the Fisher-Snedecor $\mathcal{F}$ model covers several fading distributions as special cases [9].

Let $X \sim FTR(m, K, \sigma^2, \Delta)$. The PDF and CDF of X can be expressed, respectively, as follows [10]:

$$f_X(x) = \frac{m^m}{\Gamma(m)} \sum_{j=0}^{M} \frac{K^j \alpha_j}{j!} \frac{x^j}{\Gamma(j+1)(2\sigma^2)^{j+1}} \exp\left(-\frac{x}{2\sigma^2}\right), \quad (1)$$

$$F_X(x) = \frac{m^m}{\Gamma(m)} \sum_{j=0}^{M} \frac{K^j \alpha_j}{j!} \frac{1}{\Gamma(j+1)} \gamma\left(j+1, \frac{x}{2\sigma^2}\right), \quad (2)$$

where

$$\alpha_j = \sum_{k=0}^{j} \binom{j}{k} \sum_{l=0}^{k} \binom{k}{l} \Gamma(j+m+2l-k)(m+K)^{k-j-m-2l} \times K^{2l-k} \left(\frac{\Delta}{2}\right)^{2l} (-1)^{2l-k} R_{j+m}^{k-2l}\left(\left[\frac{K\Delta}{m+K}\right]^2\right), \quad (3)$$

$$R_\upsilon^\mu(x) = \begin{cases} \frac{\left(\frac{\upsilon-\mu}{2}\right)\left(\frac{\upsilon-\mu+1}{2}\right)}{\mu!} x^\mu {}_2F_1\left(\frac{\upsilon+\mu}{2}, \frac{\upsilon+\mu+1}{2}; 1+\mu; x\right), \mu \in N, \\ \frac{{}_2F_1\left(\frac{\upsilon-\mu}{2}, \frac{\upsilon-\mu+1}{2}; 1-\mu; x\right)}{\Gamma(1-\mu)}, \text{otherwise}, \end{cases} \quad (4)$$

and M is a large constant that satisfies $\sum_{j=0}^{M} \alpha_j \to 1$. Typically, to obtain a satisfactory accuracy, e.g., $1 - \sum_{j=0}^{M} \alpha_j < 10^{-6}$, only less than 30 terms are needed [11], which is easy to compute.

Let $Z \sim \mathcal{F}(m_f, m_s, \bar{z})$, the PDF and CDF of the squared $\mathcal{F}$ RV Z can be written as [12]

$$f_Z(z) = \frac{{m_f}^{m_f}(m_s-1)^{m_s} \bar{z}^{m_s} z^{m_f-1}}{B(m_f, m_s)(m_f z + (m_s-1)\bar{z})^{m_f+m_s}}, \quad (5)$$

and

$$F_Z(z) = \frac{z^{m_f} {}_2F_1\left(m_f, m_f+m_s, m_f+1; -\frac{m_f z}{(m_s-1)\bar{z}}\right)}{{m_f}^{1-m_f} B(m_f, m_s)(m_s-1)^{m_f} \bar{z}^{m_f}}. \quad (6)$$

C. SINR Analysis

We consider that K antennas in UAV are used to serve K users on orthogonal channels. Therefore, the signal received by the user U_k can be expressed as $y_k = \sqrt{P_{ak}} h_{ak} s_k + n + \sqrt{P_{jk}} h_{jk}$, where P_{ak} denotes the transmit power of the antenna which operates on the k_{th} channel, h_{ak} is the channel coefficient from UAV to user U_k, s_k denotes the data of user U_k, $\|s_k\|^2 = 1$, P_{jk} is the jamming power allocated to user U_k, h_{jk} is the channel coefficient form jammer to user U_k, and n is the additive white Gaussian noise (AWGN) at the user with $n \sim \mathcal{CN}(0, \kappa^2)$. We denote the maximal sum transmit and jamming power by P_T and P_J, respectively. We can express the SINR of user U_k as

$$\gamma_k = \frac{D_{ak}^{-\alpha_{ak}} P_{ak} h_{ak}^2}{\kappa^2 + D_{jk}^{-\alpha_{jk}} P_{jk} h_{jk}^2} \triangleq \frac{C_{1k} X_k}{\kappa^2 + C_{2k} Z_k}, \quad (7)$$

[1] Our analysis can be generalized to the case of multi-antennas serving one user [7]. The reason is that FTR fading is used to model the small-scale fading in air-to-ground links (see Section II-B), which can be regarded as the approximation to the distribution of the sum of FTR RVs [7].

$$\xi_k = 1 - \frac{{m_{fw}}^{m_{fw}-1}\left(\varepsilon_k-\kappa^2\right)^{m_{fw}}}{{C_{2w}}^{m_{fw}} B\left(m_{fw},m_{sw}\right)\left(m_{sw}-1\right)^{m_{fw}} \bar{z}_w^{m_{fw}}} {}_2F_1\left(m_{fw}, m_{fw}+m_{sw}, m_{fw}+1; -\frac{m_{fw}\left(\varepsilon_k-\kappa^2\right)}{\Omega_w}\right)$$
$$- \frac{{m_w}^{m_w}}{\Gamma\left(m_{fw}\right)\Gamma\left(m_{sw}\right)\Gamma\left(m_w\right)} \sum_{j=0}^{M} \frac{{K_w}^j \alpha_{wj}}{j!\Gamma(j+1)} G_{1,0:2,3:1,1}^{0,0:2,2:1,1}\left(\begin{matrix} 0 \\ - \end{matrix} \middle| \begin{matrix} 1, 1-m_{fw} \\ m_{sw}, 1, 0 \end{matrix} \middle| \begin{matrix} -j \\ 0 \end{matrix} \middle| \frac{\Omega_w}{m_{fw}\left(\varepsilon_{th}-\kappa^2\right)}, \frac{2C_{1w}\sigma_w^2}{\varepsilon_{th}-\kappa^2} \right) \tag{9}$$

$$R_k = \frac{-{m_k}^{m_k}}{\ln 2\Gamma\left(m_k\right)\Gamma\left(m_{fk}\right)\Gamma\left(m_{sk}\right)} \left(\frac{m_{fk}\kappa^2}{\Omega_k}\right)^{m_{fk}} \sum_{j=0}^{M} \frac{{K_k}^j \alpha_{kj}}{\Gamma\left(j+1\right) j!}$$
$$\times G_{1,0:0,3:1,2}^{0,0:3,1:2,1}\left(\begin{matrix} 1-m_{sk}-m_{fk} \\ - \end{matrix} \middle| \begin{matrix} 1 \\ m_{sk}, 1+j, 0 \end{matrix} \middle| \begin{matrix} 1 \\ m_{sk}+m_{fk}, m_{fk} \end{matrix} \middle| \frac{\kappa^2}{2\sigma_k^2}\frac{1}{C_{1k}}, \frac{\Omega_k}{m_{fk}\kappa^2-\Omega_k} \right) \tag{10}$$

where $X_k \triangleq h_{ak}^2 \sim FTR\left(m_k, K_k, {\sigma^2}_k, \Delta_k\right)$, $Z_k \triangleq h_{jk}^2 \sim \mathcal{F}\left(m_{fk}, m_{sk}, \bar{z}_k\right)$, α_{ai} $(i \in \{k, w\})$ denotes the path loss exponents of the UAV-user U_k link and the UAV-Warden link, respectively, and α_{ji} $(i = k, w)$ are the path loss exponents of the Jammer-user U_k link and the Jammer-Warden link.

III. Covert Performance Metrics and Analysis

The warden has a binary choice between the null hypothesis, $\mathcal{H}_0$, that UAV is silent, and the alternate hypothesis, $\mathcal{H}_1$, that UAV is transmitting. The received signals at the warden's k_{th} antenna can be expressed as

$$y_{wk} = \begin{cases} \kappa^2 + D_{jw}^{-\alpha_{jw}} P_{jk} h_{jw}^2, & \mathcal{H}_0, \\ D_{aw}^{-\alpha_{aw}} P_{ak} h_{aw}^2 + \kappa^2 + D_{jw}^{-\alpha_{jw}} P_{jk} h_{jw}^2, & \mathcal{H}_1, \end{cases} \tag{8}$$

The warden's decisions are based on a threshold-based rule, which is commonly adopted [2] and advocates $\mathcal{D}_1$ and $\mathcal{D}_0$ when the received power is larger and not larger than a predefined threshold, respectively. Note that the covertness of communication is guaranteed if the warden's detection error for each user is always larger than a threshold which is arbitrarily close to 1.

A. Detection Error Probability

The warden's detection error probability can be defined as $\xi_k = \mathbb{P}_{FA} + \mathbb{P}_{MD}$, where $\mathbb{P}_{FA} = \mathbb{P}(\mathcal{D}_1|\mathcal{H}_0)$ denotes the false alarm probability, and $\mathbb{P}_{MD} = \mathbb{P}(\mathcal{D}_0|\mathcal{H}_1)$ denotes the miss detection probability.

Theorem 1. *The detection error probability is derived as* (9)*, shown at the top of the next page, where* $C_{1w} \triangleq D_{aw}^{-\alpha_{aw}} P_{ak}$*,* $C_{2w} \triangleq D_{jw}^{-\alpha_{jw}} P_{jk}$*,* ε_k *denote the detection threshold for user* U_k*, and* $\Omega_w \triangleq \left(m_{sw}-1\right) \bar{z}_w C_{2w}$*.*

Proof: Please refer to Appendix A. ∎

B. Covert Communication Rate

Theorem 2. *In our considered system, the covert rate of the* k*-th user is given by* (10)*, shown at the top of the next page, where* $\Omega_k \triangleq \left(m_{sk}-1\right) \bar{z}_k C_{2k}$*.*

Proof: Please refer to Appendix B. ∎

IV. Problem Formulation

A. Optimal Detection Threshold at Warden

We introduce the PSO algorithm for the warden to obtain the optimal threshold, denoted by Algorithm 1, in which n particles travel in an L-dimensional search space [13]. In our case, L is equal to 1. The velocity v_i and position x_i of the i_{th} particle are updated using

$$v_i\left(k+1\right) = \omega v_i\left(k\right) + c_1 R_1 \left(p_i\left(k\right) - x_i\left(k\right)\right) + c_2 R_2 \left(p_g\left(k\right) - x_i\left(k\right)\right), \tag{11}$$

and

$$x_i\left(k+1\right) = x_i\left(k\right) + v_i\left(k+1\right), \tag{12}$$

for $i = 1, 2, \ldots, m$, where ω is the inertia weight, c_1 and c_2 are acceleration constants, both R_1 and R_2 are uniformly distributed in $[0, 1]$, p_i and p_g are the best previous and global positions, respectively. To minimize ξ_k by adjusting ε_k, the warden can initialize n particles to search for the optimal detection threshold, ε_k^{opt}. The total running time can be expressed as $n\text{M}_{\text{PSO}}T_T$, where T_T is the time required by per particle in one iteration [14].

B. Game Theoretic Problem Formulation

In games, K users aim to reach an agreement that is efficient and fair given the five axioms of PAR, IR, INV, IIA and SYM [4]. In our case, the resource is the transmitting and jamming power, and the utility function of user U_k can be defined as $U_k\left(P_{ak}, P_{jk}\right)$. The NBS can give a fair solution for the NBG [4]. With the help of NBS, our problem can be formulated as

$$\max_{\{P_{jk}, P_{ak}\}} \quad \prod_{k=1}^{K} \left(R_k - R_k^{\text{th}}\right) \tag{13a}$$
$$\text{s.t.} \quad \sum_{k=1}^{K} P_{jk} \leqslant P_J, \tag{13b}$$
$$\sum_{k=1}^{K} P_{ak} \leqslant P_T, \tag{13c}$$
$$\xi_k \geqslant \xi_k^{\text{th}}, \forall k, \tag{13d}$$

where R_k can be calculated as in (10), ξ_k^{th} is a constant which is close to 1, and ξ_k can be obtained by (9) under the optimal detection threshold. Note that our problem and solution are equivalent to standard Nash bargaining problem, and hence these five axioms that mentioned before are achievable intrinsically.

V. Joint Jamming and Transmitting Power Allocation Algorithm

A. Converge Analysis

Note that the power constraints, (13b) and (13c), are convex with respect to P_{jk} and P_{ak}, respectively. For (13d), the Hessian matrix can be expressed as

$$\nabla^2 \xi_k = \begin{vmatrix} \frac{\partial^2 \xi_k}{\partial {C_{1w}}^2} & \frac{\partial^2 \xi_k}{\partial C_{1w} \partial C_{2w}} \\ \frac{\partial^2 \xi_k}{\partial C_{2w} \partial C_{1w}} & \frac{\partial^2 \xi_k}{\partial {C_{2w}}^2} \end{vmatrix}. \tag{14}$$

We can analyze the Hessian matrix of ξ_k is semi-negative definite (See Appendix C), which means that the constraint set is convex. By regarding (9) as the fitness function, PSO can be used to obtain the maximum ξ_k and corresponding ε_k because the search space is convex.

B. PSO-based Power Allocation Algorithm

We can observe that (13b)-(13d) actually limit the ranges of P_{ak} and P_{jk}, which can be regarded as the boundary to PSO's search space. In the following, we propose a PSO-based algorithm, denoted by Algorithm 2, under the particles' location limitation given in (13b)-(13d). The output now is the optimal transmit and jamming power allocation, $\{P_{j1}^{opt}, \ldots, P_{jK}^{opt}\}$ and $\{P_{a1}^{opt}, \ldots, P_{aK}^{opt}\}$, the fitness function is $\prod_{k=1}^{K} \left(R_k - R_k^{\text{th}}\right)$, and the dimension of searching space is $2K$ because the $2K$ coordinates of each particle represent one possible transmit and jamming power allocation scheme. The total running time of Algorithm 2 is $T_P = 2nKT_T \text{M}_{\text{PSO}}$, where T_T denotes the time required by per particle in one iteration, M_{PSO} is the iteration number, and n denotes the size of swarm.

VI. Numerical Results

In this section, simulation results are presented to verify the proposed analysis. We set $K = 3$, and the locations of the three users, the jammer, the UAV, and the warden are $\mathbf{q}_1 = [0, 10, 0]^T$, $\mathbf{q}_2 = [7, 14, 0]^T$, $\mathbf{q}_3 = [5, 20, 0]^T$, $\mathbf{q}_j = [7, 24, 0]^T$, $\mathbf{q}_a = [5, 13, 20]^T$, and $\mathbf{q}_w = [5, 16, 0]^T$, respectively. The AWGN power is $\kappa^2 = 3$ dB. For parameters of Fisher-Snedecor $\mathcal{F}$ fading model, we set $m_{f1} = 2$, $m_{f2} = 3$, $m_{f3} = 5$, $m_{fw} = 3$, $m_{s1} = 4$, $m_{s2} = 4$, $m_{s3} = 5$, $m_{sw} = 4$, $\bar{z}_1 = -10$ dB, $\bar{z}_2 = -12$ dB, $\bar{z}_3 = -13$ dB, and $\bar{z}_w = -11$ dB. For parameters of FTR fading model, we set $m_1 = 4$, $m_2 = 3$, $m_3 = 5$, $m_w = 4$, $K_1 = 4$, $K_2 = 5$, $K_3 = 5$, $K_w = 3$, $\Delta_1 = 0.5$, $\Delta_2 = 0.5$, $\Delta_3 = 0.4$, $\Delta_w = 0.4$, $2\sigma_1^2(1 + K_1) = -10$ dB, $2\sigma_2^2(1 + K_2) = -15$ dB, $2\sigma_3^2(1 + K_3) = -11$ dB, and $2\sigma_w^2(1 + K_w) = -10$ dB.

Figure 2 shows the detection error probability, ξ_k $(k = 1, 2, 3)$, versus the detection threshold with or without our proposed PPA algorithm, with $P_T = 20$ dB, $P_J = 20$ dB, and $\xi_k^{\text{th}} = 95\%$. With the help of Algorithm 1, the optimal detection threshold for each user obtained by the warden is marked with stars. As shown by the dotted lines, all users' communication can make the warden's detection error probability reach more than 95% and be turned into secure ones, even under the warden's optimal detection threshold.

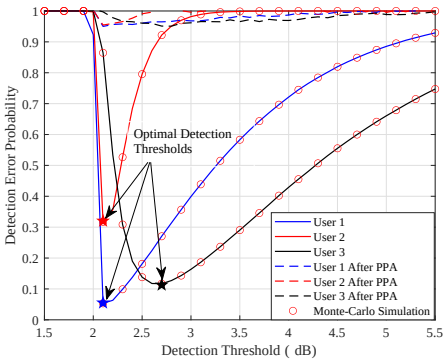

Fig. 2. The detection error probability, ξ_k $(k = 1, 2, 3)$, versus the detection threshold with or without our proposed PPA algorithm, with $P_T = 20$, $P_J = 20$, and $\xi_k^{\text{th}} = 95\%$.

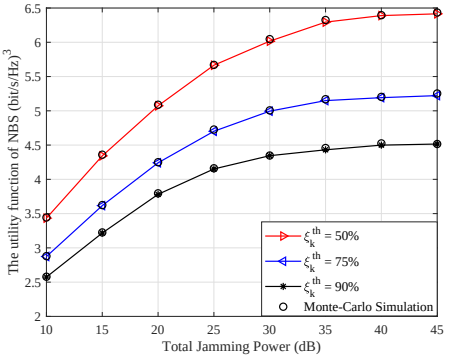

Fig. 3. The NBS's utility function versus with the jammer's available total power under the different detection error thresholds, with $P_T = 30$ dB.

Specifically, the error probabilities of users U_k $(k = 1, 2, 3)$ increase 1800%, 196% and 691%, respectively. These results demonstrate the effectiveness of our proposed algorithm.

Figure 3 depicts the NBS's utility function versus the jammer's available total power under the different detection error thresholds, with $P_T = 20$ dB. More specifically, we can observe that the utility function increases by 78% when P_J increases from 10 dB to 30 dB with $\xi_k^{\text{th}} = 75\%$. Another insight is that the utility is higher when the ξ_k^{th} is lower. For example, when ξ_k^{th} decreases from 90% to 50% with $P_J = 30$ dB, the utility function increases by 39%. The reason is that a high ξ_k^{th} means that the system has high requirements for covertness. Thus, the UAV has to allocate lower transmit power to users to meet the covertness requirements. In contrast, we can deploy a higher UAV's transmit power P_T to enhance the system's utility when the jammer has sufficient power to dramatically degrade the warden's detection capability.

Fig. 4 shows the NBS's utility function versus theP_T, under different sets of P_J, with $\xi_k^{\text{th}} = 90\%$. It is interesting that when the total transmit power is small, the utility functions at different total jamming powers are very close to each other. The reason is that the jamming power required to achieve a

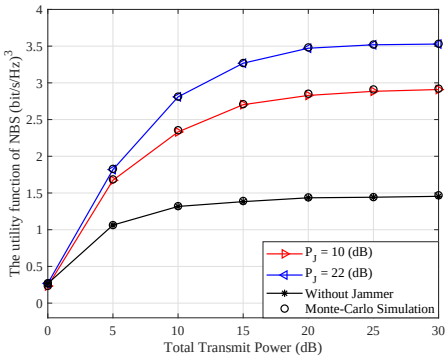

Fig. 4. The NBS's utility function versus the total transmit power of UAV, under different sets of total transmit powers of UAV, with $\xi_k^{\text{th}} = 90\%$.

high detection error probability is low when the transmit power is low. When the total transmit power is larger, we can observe that the difference between utility functions under different total jamming power is larger. For example, when $P_T = 30$ dB, the utility function increases 22% when P_J increases from 10 dB to 20 dB. The case without jammer is also shown in Fig. 4. We can observe that the utility achieved with the help of jammer is significantly larger.

VII. Conclusion

A jammer-aided multi-antenna UAV covert communication system is investigated. We used the Fisher-Snedecor $\mathcal{F}$ and FTR fading to derive the exact important performance metrics including detection error probability and covert rate. Furthermore, we formulated the joint transmit and jamming power allocation problem as a NBG to maximize the user's covert rate with limited transmit and jamming power and ensure the covertness of communication simultaneously. To solve the formulated problem, we proposed a PPA algorithm, under the warden's optimal detection threshold. PSO were used by the warden in finding the optimal detection threshold. Numerical results illustrated that the jammer's total power and the UAV's transmit power can be jointly allocated to improve the covert rate, and our proposed algorithms are effective.

Appendix A
Proof of Theorem 1

For the term of $\mathbb{P}_{AF}$, we have $\mathbb{P}_{AF} = \Pr\left(\kappa^2 + C_{2w}Z_w > \varepsilon_k\right)$. Denote that $T_w \triangleq \kappa^2 + C_{2w}Z_w$, and we can derive the CDF of T_w as $F_{T_w}(t) = F_{Z_w}\left(\frac{t-\kappa^2}{C_{2w}}\right)$, where $Z_w \triangleq h_{jw}^2$. Thus, $\mathbb{P}_{AF}$ can be expressed as $\mathbb{P}_{AF} = 1 - F_{Z_w}\left(\frac{\varepsilon_k-\kappa^2}{C_{2w}}\right)$. On the other hand, for the term of $\mathbb{P}_{MD}$, we have $\mathbb{P}_{MD} = \Pr\left(T_w + C_{1w}X_w < \varepsilon_k\right)$. Let $Y_w = X_w + Z_w$. The CDF of Y_w can be expressed as $F_{Y_w}(y) = \int_0^\infty F_{T_w}(y-t)\frac{1}{C_{1w}}f_{X_w}\left(\frac{t}{C_{1w}}\right)\mathrm{d}t$. With the help of [5, eq. (9.113)], [5, eq. (8.331.1)] and [15, eq. (01.03.07.0001.01)], [5, eq. (3.194.3)] and [5, eq. (8.384.1)], F_{Y_w} can be solved. With the help of [6, eq. (1)], we can derive $\mathbb{P}_{MD}$ as $P_{MD} = \Pr\left(\kappa^2 + C_{1w}X_w + C_{2w}Z_w < \varepsilon_k\right) = F_Y(\varepsilon_k)$, which completes the proof.

Appendix B
Proof of Theorem 2

The covert rate can be derived as $R_k = \int_0^\infty \log(1+\gamma) f_{\gamma_k}(\gamma)\,\mathrm{d}\gamma$. Let $U_k \triangleq \frac{\gamma_k}{C_{1k}} = \frac{X_k}{T_k}$, where $T_k \triangleq \kappa^2 + P_{jk}Z_k$. The PDF of T_k can be expressed as $f_{T_k}(t) = \frac{1}{C_{2k}}f_Z\left(\frac{t-\kappa^2}{C_{2k}}\right)$. With the help of (1), we can obtain the PDF of U as

$$f_{U_k}(u) = \int_0^\infty x f_{X_k}(ux) f_{T_k}(x)\,\mathrm{d}x = \frac{{m_k}^{m_k}}{\Gamma(m_k)}\sum_{j=0}^{M}\frac{{K_k}^j\alpha_{kj}}{j!} \times \frac{u^j {m_{fk}}^{m_{fk}}(m_{sk}-1)^{m_{sk}}\bar{z}_k^{m_{sk}}}{\Gamma(j+1)\left(2\sigma_k^2\right)^{j+1}{C_{2k}}^{m_{fk}}B(m_{fk},m_{sk})}I_B, \quad \text{(B-1)}$$

where

$$I_B = \int_0^\infty \frac{x^{j+1}\left(x-\kappa^2\right)^{m_{fk}-1}\exp\left(-\frac{ux}{2\sigma_k^2}\right)}{\left(\frac{m_{fk}x}{P_{jk}} - \frac{m_{fk}\kappa^2}{P_{jk}} + (m_{sk}-1)\bar{z}_k\right)^{m_{fk}+m_{sk}}}\mathrm{d}x. \quad \text{(B-2)}$$

With the help of [15, eq. (01.03.07.0001.01)], [5, eq. (3.197.1)], [5, eq. (9.113)] and [5, eq. (8.384.1)], the integration part in I_B can be solved. With the help of [6, eq. (1)], and $f_\gamma(\gamma) = \frac{1}{C_{1k}}f_U\left(\frac{\gamma}{C_{1k}}\right)$, we can derive (B-3).

With the help of (B-3), [16, eq. (2.6.9.21)] and [5, eq. (8.334.3)], we can obtain (10), which completes the proof.

Appendix C
Proof about Hessian matrix of ξ_k

We first prove that the $I_L \triangleq \int_0^\infty t^A(B-t)^C\exp(-Dt)\mathrm{d}t$ can be approximated as $I_L \approx D^{-A-1}B^C\Gamma(A+1)$. Let T denote a constant that is close to zero. We have $I_L \approx \lim_{T\to 0}\int_T^\infty t^A(B-t)^C\exp(-Dt)\,\mathrm{d}t$. Using [15, eq. (01.03.07.0001.01)] and exchanging the order of integration, we can express I_L as $I_L = \lim_{T\to 0}\frac{D^s}{2\pi i}\int_{\mathcal{L}}\Gamma(-s)I_D ds$. With the help of [5, eq. (3.194.2)] and [5, eq. (9.113)], I_D can be solved. Substitute I_D into I_L, we obtain

$$I_L = \lim_{T\to 0}\frac{D^{-A-1}}{(2\pi i)^2}\int_{\mathcal{L}_1}\int_{\mathcal{L}_2}\left(-\frac{B}{T}\right)^{s_2}\left(\frac{T}{D}\right)^{s_1}\Gamma(-C-s_1+s_2) \times \frac{\Gamma(-s_1+A+1)\Gamma(-C+s_2)\Gamma(-s_2)}{(-T)^{-C}\Gamma(-C)\Gamma(1-C-s_1+s_2)}\mathrm{d}s_2\mathrm{d}s_1, \quad \text{(C-1)}$$

where the integration path of $\mathcal{L}_1$ goes from $\sigma_{L1}-i\infty$ to $\sigma_{L1}+i\infty$ and the integration path of $\mathcal{L}_2$ goes from $\sigma_{L2}-i\infty$ to $\sigma_{L2}+i\infty$. When $T\to 0$, we have $-\frac{B}{T}\to-\infty$ and $TD\to 0$. With the help of [17, Theorem 1.11], the Mellin-Barnes integral over $\mathcal{L}_1$ can be approximated by evaluating the residue at the minimum pole on the right hand side of σ_{L1} and the Mellin-Barnes integral over $\mathcal{L}_2$ can be approximated by evaluating the residue at the minimum pole on the left hand side of σ_{L2}. Thus, using [5, eq. (8.331.1)] and [5, eq. (8.338.1)], we have $I_L \approx D^{-A-1}B^C\Gamma(A+1)$, which completes the proof.

With the help of [5, eq. (9.100)] and [5, eq. (1.211.1)], we can rewrite ξ_k as (C-2), shown at the top of the next page, where $I_J = \int_0^\infty t^{j+p}\left(\varepsilon_k - \kappa^2 - t\right)^{q+m_{fw}}\mathrm{d}t$.

$$f_{\gamma_k}(\gamma)=\frac{{m_k}^{m_k}\Gamma^{-1}(m_k)}{\gamma\Gamma\left(m_{fk}\right)\Gamma(m_{sk})}\left(\frac{m_{fk}\kappa^2}{\Omega_k}\right)^{m_{fk}}\sum_{j=0}^{M}\frac{{K_k}^j\alpha_{kj}}{\Gamma(j+1)\,j!}G_{1,0:0,2:1,2}^{0,0:2,0:2,1}\left(\begin{matrix}1-m_{sk}-m_{fk}\\-\end{matrix}\middle|\begin{matrix}-\\m_{sk},1+j\end{matrix}\middle|\begin{matrix}1\\m_{sk}+m_{fk},m_{fk}\end{matrix}\middle|\frac{\gamma\kappa^2}{2C_{1k}\sigma_k^2},\frac{\Omega_k}{m_{fk}\kappa^2-\Omega_k}\right) \tag{B-3}$$

$$\xi_k=1-\frac{{m_{fw}}^{m_{fw}-1}\left(\varepsilon_k-\kappa^2\right)^{m_{fw}}}{B\left(m_{fw},m_{sw}\right)\left(m_{sw}-1\right)^{m_{fw}}\bar{z}_w^{m_{fw}}}\sum_{q=0}^{\infty}\frac{\left(m_{fw}\right)_q\left(m_{fw}+m_{sw}\right)_q}{\left(m_{fw}+1\right)_q q!}\left(-\frac{m_{fw}\left(\varepsilon_k-\kappa^2\right)}{\left(m_{sw}-1\right)\bar{z}_w}\right)^q\frac{1}{C_{2w}^{q+m_{fw}}}+\frac{{m_{fw}}^{m_{fw}-1}}{B\left(m_{fw},m_{sw}\right)\left(m_{sw}-1\right)^{m_{fw}}\bar{z}_w^{m_{fw}}}$$
$$\times\frac{{m_w}^{m_w}}{\Gamma\left(m_w\right)}\sum_{j=0}^{\infty}\frac{{K_w}^j\alpha_{wj}}{j!}\frac{1}{\Gamma\left(j+1\right)\left(2\sigma_w^2\right)^{j+1}}\sum_{p=0}^{\infty}\frac{1}{p!}\left(\frac{-1}{2\sigma_w^2}\right)^p\sum_{q=0}^{\infty}\frac{\left(m_{fw}\right)_q\left(m_{fw}+m_{sw}\right)_q}{\left(m_{fw}+1\right)_q q!}\left(\frac{-m_{fw}}{\left(m_{sw}-1\right)\bar{z}_w}\right)^q\frac{1}{C_{1w}^{p+j+1}}\frac{1}{C_{2w}^{q+m_{fw}}}I_J \tag{C-2}$$

With the help of [5, eq. (3.383.1)], [5, eq. (8.384.1)], and [15, eq. (07.20.07.0004.01)], after some algebraic manipulations, proving $\frac{\partial^2\xi_k}{\partial {C_{2w}}^2}<0$ is equivalent to prove that

$$F_2(C_{1w})\triangleq\frac{{m_w}^{m_w}}{\Gamma\left(m_w\right)}\sum_{j=0}^{M}\frac{{K_w}^j\alpha_{wj}}{j!}\frac{\Gamma\left(m_w+q+1\right)}{\Gamma\left(j+1\right)}\frac{1}{2\pi i}$$
$$\times\int_{\mathcal{L}}\frac{\Gamma\left(t+j+1\right)\Gamma\left(-t\right)}{\Gamma\left(m_w+q+1-t\right)}\left(\frac{2C_{1w}\sigma_w^2}{\varepsilon_k^{opt}-\kappa^2}\right)^t\mathrm{d}t<1, \tag{C-3}$$

where the integration path of $\mathcal{L}$ goes from $\sigma_L-i\infty$ to $\sigma_L+i\infty$ and $\sigma\in\mathbb{R}$. When $C_{1w}\to\infty$, we have $F_2(C_{1w})\to 0$, which means that there must exist C'_{1w} such that when C_{1w} is greater than C'_{1w}, we always have $\frac{\partial^2\xi_k}{\partial {C_{2w}}^2}<0$. This is reasonable because the UAV transmit power allocated to users should be large enough to meet the QoS requirements. Users may quit gaming if their data rate is too low. With the help of (C-2), we can observe that $\frac{\partial^2\xi_k}{\partial C_{1w}\partial C_{2w}}\times\frac{\partial^2\xi_k}{\partial C_{2w}\partial C_{1w}}>0$ and $\frac{\partial^2\xi_k}{\partial {C_{1w}}^2}>0$. Thus, we have $\nabla^2\xi_k=\frac{\partial^2\xi_k}{\partial {C_{1w}}^2}\frac{\partial^2\xi_k}{\partial {C_{2w}}^2}-\frac{\partial^2\xi_k}{\partial C_{1w}\partial C_{2w}}\frac{\partial^2\xi_k}{\partial C_{2w}\partial C_{1w}}<0$, which completes the proof.

References

[1] Z. Lin, M. Lin, T. de Cola, J.-B. Wang, W.-P. Zhu, and J. Cheng, "Supporting iot with rate-splitting multiple access in satellite and aerial-integrated networks," *IEEE Internet Things J.*, vol. 8, no. 14, pp. 11 123–11 134, Jan. 2021.

[2] X. Jiang, X. Chen, J. Tang, N. Zhao, X. Y. Zhang, D. Niyato, and K.-K. Wong, "Covert communication in UAV-assisted air-ground networks," *IEEE Wireless Commun.*, to appear, 2021.

[3] M. J. Osborne and A. Rubinstein, *A course in game theory*. MIT press, 1994.

[4] J. F. Nash, "The bargaining problem," *Econometrica, J. Econ. Soc.*, vol. 18, no. 2, pp. 155–162, 1950.

[5] I. S. Gradshteyn and I. M. Ryzhik, *Table of Integrals, Series, and Products*, 7th ed. Academic Press, 2007.

[6] B. L. Sharma and R. F. A. Abiodun, "Generating function for generalized function of two variables," *Proc. American Mathematical Society*, vol. 46, no. 1, pp. 69–72, Oct. 1974.

[8] J. M. Romero-Jerez, F. J. Lopez-Martinez, J. F. Paris, and A. J. Goldsmith, "The fluctuating two-ray fading model: Statistical characterization and performance analysis," *IEEE Trans. Wireless Commun.*, vol. 16, no. 7, pp. 4420–4432, Jul. 2017.

[7] J. Zhang, H. Du, P. Zhang, J. Cheng, and L. Yang, "Performance analysis of 5G mobile relay systems for high-speed trains," *IEEE J. Select. Areas Commun.*, vol. 38, no. 12, pp. 2760–2772, Dec. 2020.

[9] S. K. Yoo, S. L. Cotton, P. C. Sofotasios, M. Matthaiou, M. Valkama, and G. K. Karagiannidis, "The Fishe-Snedecor $\mathcal{F}$ distribution: A simple and accurate composite fading model," *IEEE Commun. Lett.*, vol. 21, no. 7, pp. 1661–1664, Jul. 2017.

[10] J. Zhang, W. Zeng, X. Li, Q. Sun, and K. P. Peppas, "New results on the fluctuating two-ray model with arbitrary fading parameters and its applications," *IEEE Trans. Veh. Technol.*, vol. 67, no. 3, pp. 2766–2770, Mar. 2017.

[11] J. Zheng, J. Zhang, G. Pan, J. Cheng, and B. Ai, "Sum of squared fluctuating two-ray random variables with wireless applications," *IEEE Trans. Veh. Technol.*, vol. 68, no. 8, pp. 8173–8177, Aug. 2019.

[12] S. K. Yoo, P. C. Sofotasios, S. L. Cotton, S. Muhaidat, F. J. Lopez-Martinez, J. M. Romero-Jerez, and G. K. Karagiannidis, "A comprehensive analysis of the achievable channel capacity in $\mathcal{F}$ composite fading channels," *IEEE Access*, vol. 7, pp. 34 078 – 34 094, Mar. 2019.

[13] S. Cheng, H. Lu, X. Lei, and Y. Shi, "A quarter century of particle swarm optimization," *Complex Intell. Syst.*, vol. 4, no. 3, pp. 227–239, Mar. 2018.

[14] A. Chraibi, S. B. Alla, A. Touhafi, and A. Ezzati, "Run time optimization using a novel implementation of parallel-PSO for real-world applications," in *Proc. 5th CloudTech*, May 2020, pp. 1–7.

[15] Wolfram, "The wolfram functions site," http://functions.wolfram.com.

[16] A. P. Prudnikov, J. A. Bryčkov, and O. I. Maričev, *Integrals and Series. Vol. 1, Elementary Function*, 1986.

[17] A. M. Mathai, R. K. Saxena, and H. J. Haubold, *The H-function: Theory and Applications*. Springer Science & Business Media, 2009.